



## A=104-107核反应堆裂变产物的 $\beta$ 衰变 全吸收谱学研究

报告人：帅 鹏





- 全吸收谱仪的研究领域和应用
- 模块化全吸收谱仪（MTAS）
- $A=104, 105, 107$ 的 $\beta$ 衰变全吸收谱学
- 总结和展望

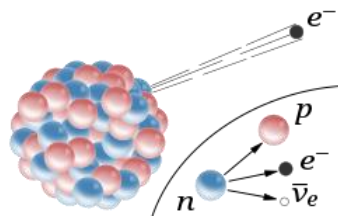
## 核物理

核结构：  
衰变强度,形变

$$B(\text{GT})^\beta = \frac{K}{\lambda^2} \frac{I_\beta(E)}{f(Q_\beta - E, Z) T_{1/2}}$$

核天体r过程：  
 $T_{1/2}$ ,  $\beta_{\text{xn}}$ ,  $\beta$ -oslo

$\beta$  衰变电子能谱：  
形状因子



$Q_\beta$   
半衰期  $T_{1/2}$   
 $\beta$  缓发中子  $P_n$   
真实  $\beta$  衰变分支比  $I_\beta$

## 核反应堆

核反应堆：  
中微子反常

反应堆安全：  
衰变热

超越标准模型：  
Sterile neutrino

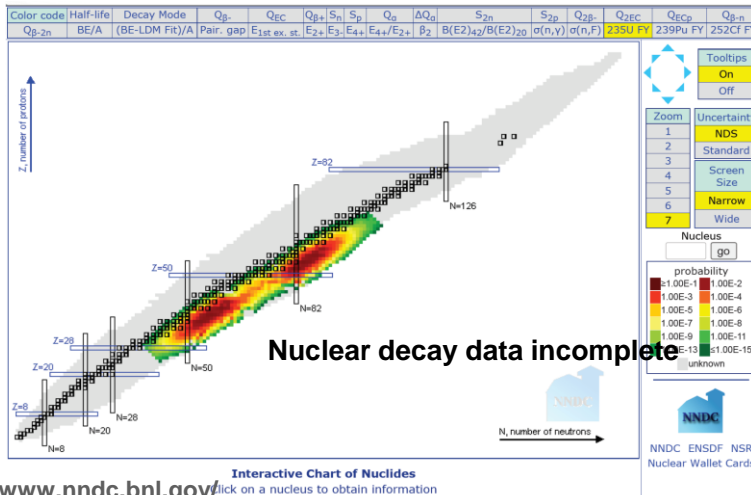


# 核反应堆 $\beta$ 衰变热



Reactor science: decay heat and antineutrino flux

Mass distribution of  $^{235}\text{U}$  fission products:



Decay heat :

$\beta$  decay heat

$$I(E_b) = \sum Y_i \times I_i(E_b)$$

$\gamma$  decay heat

$$I(E_g) = \sum Y_i \times I_i(E_g)$$

i = all fission fragments

Decay heat is the energy released by the  $\beta$  decay of fission yield products.

Decay heat is **~8%** of the energy output of a nuclear reactor while it is running.

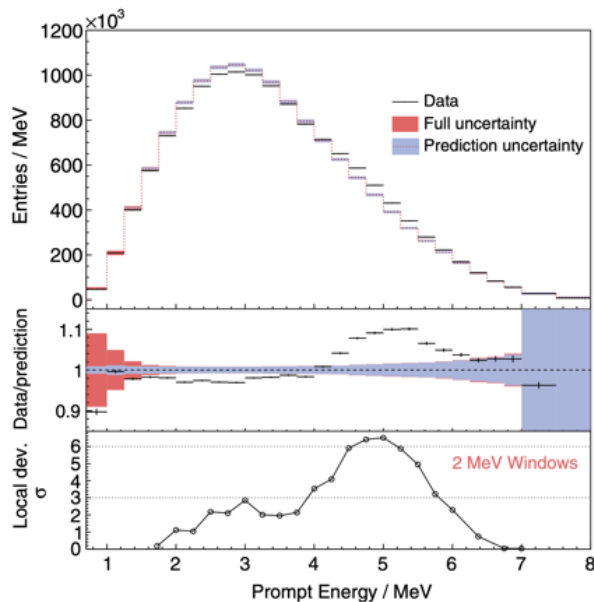
Decay heat is **100%** of the energy release after shutdown or accidental loss of cooling.

Improved knowledge of decay heat can improve fuel assembly design, future reactor design, and reactor safety.

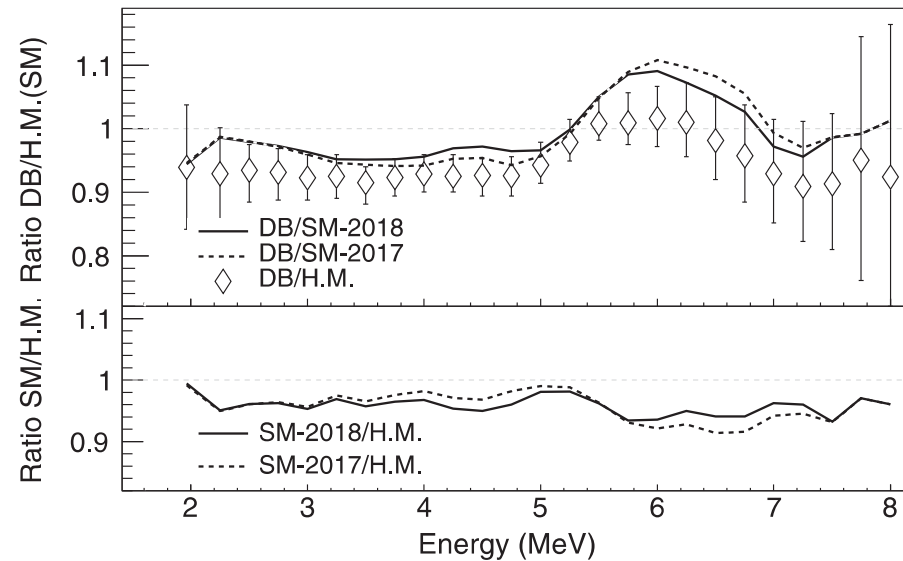
## Reactor antineutrino anomaly

Ratio of the measured reactor antineutrino spectrum to the antineutrino flux prediction.

$$0.953 \pm 0.014 (\text{exp.}) \pm 0.023 (\text{model}).$$



Daya Bay collaboration (An et al., PRL 116, 061801, 2016; An, et al., PRL 123, 111801, 2019)



M. Estienne, et al., PRL123, 022502 (2019)

**Summation method: The calculated flux obtained now lies only 1.9% above that detected in the Daya Bay experiment**

SM: A. A. Sonzogni, et al, PRC 91, 011301(R) (2015)

Huber-Mueller: Huber, PRC 84, 024617 (2011), T. A. Mueller et al., PRC 83, 054615 (2011).

Lorenzo Perisse, et al, arxiv:2304.14992 (2023)

## N-RICH PARENT (Z,N)

Hardy, et al., PLB 71, 1977

$\beta$  - transition

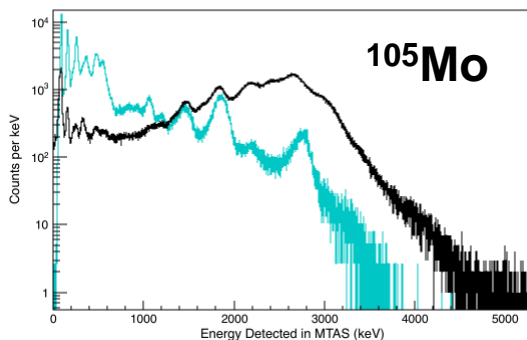
### 1. Pandemonium Effect

低探测效率的高纯锗探测器  
可能系统性地低估 $\beta$ 衰变中  
布居到高激发态的几率

$$\gamma \uparrow : \beta^- \downarrow, \bar{\nu}_e \downarrow$$



DAUGHTER (Z+1, N-1)



### 2. 基态-基态跃迁

没有与 $\beta$ 符合的 $\gamma$ ，电子探测效率对探测器的尺寸和结构非常敏感  
可能低估，也可能高估

$^{92}\text{Rb}$ :

C.M. Baglin, NDS 66, 347 (1992):

51(2)%

ENSDF 2007: 50(18)%

Rasco et al, PRL 117, 092501 (2016):

91(3)%

大量远离 $\beta$ 稳定线的丰中子核素缺乏 $\beta$ 衰变数据；  
即使是 $\beta$ 稳定线附近的核素也有必要重新测量或评估



# 国家上已有的全吸收谱仪





# 已经由实验证实的衰变数据不可靠的核素



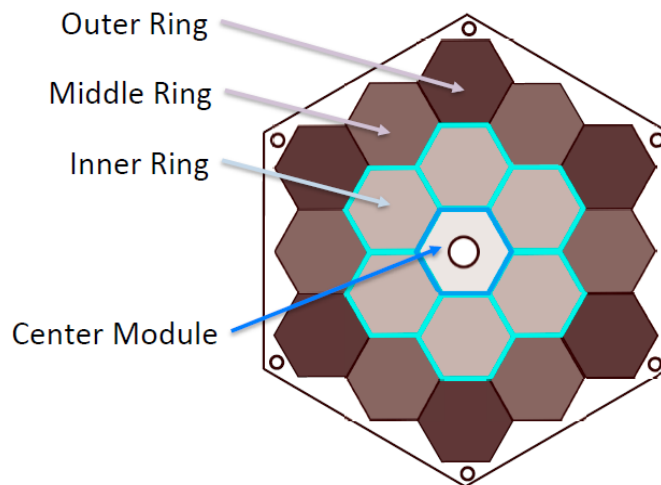
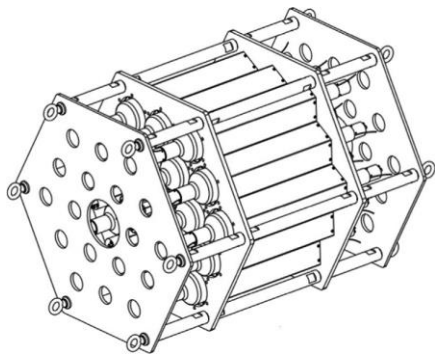
| Isotope   |
|---|
| $^{76}\text{Ga}$  |
| $^{84}\text{Br}, ^{85}\text{Br}$  |
| $^{86}\text{Br}, ^{91}\text{Rb}$  |
| $^{87}\text{Br}, ^{88}\text{Br}, ^{94}\text{Rb}$  |
| $^{89}\text{Kr}, ^{89}\text{Rb}, ^{90}\text{Kr}, ^{90}\text{Rb}, ^{90}\text{Rb}^{\text{m}}, ^{92}\text{Rb}$ |
| $^{93}\text{Rb}, ^{139}\text{Xe}$   |
| $^{94}\text{Kr}$  |
| $^{94}\text{Sr}$  |
| $^{95}\text{Rb}, ^{137}\text{I}$  |
| $^{96}\text{Y}, ^{96}\text{Y}^{\text{m}}$   |
| $^{98}\text{Nb}$  |
| $^{142}\text{Cs}$   |
| $^{100}\text{Nb}, ^{100}\text{Nb}^{\text{m}}, ^{102}\text{Nb}, ^{102}\text{Nb}^{\text{m}}$                  |
| $^{101}\text{Nb}, ^{105}\text{Mo}, ^{106}\text{Tc}, ^{107}\text{Tc}$  |
| $^{100}\text{Tc}$   |
| $^{102}\text{Tc}, ^{104}\text{Tc}, ^{105}\text{Tc}$   |
| $^{101}\text{Zr}, ^{102}\text{Zr}, ^{109}\text{Tc}$   |
| $^{103}\text{Mo}, ^{103}\text{Tc}, ^{140}\text{Cs}$   |
| $^{103}\text{Nb}, ^{104}\text{Nb}^{\text{m}}$   |
| $^{137}\text{Xe}$   |

- $Q_{\beta}$ 较大的裂变产物大部分都由TAGS技术重新测量
- 大部分受Pandemonium效应影响，小部分是基态分支比不准，如 $^{92}\text{Rb}$
- 总体降低IBD产额6-8%
- 仍有许多核素需要重新评估

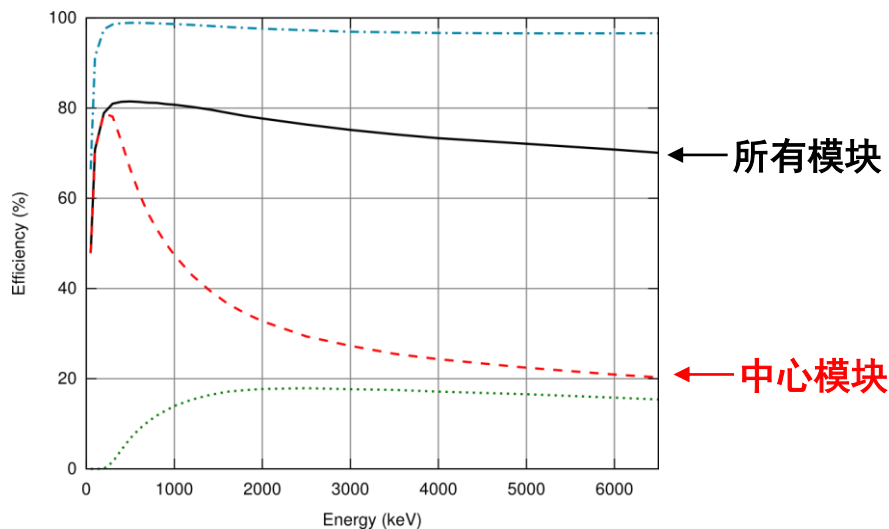
Lorenzo Perisse, et al, arxiv:2304.14992



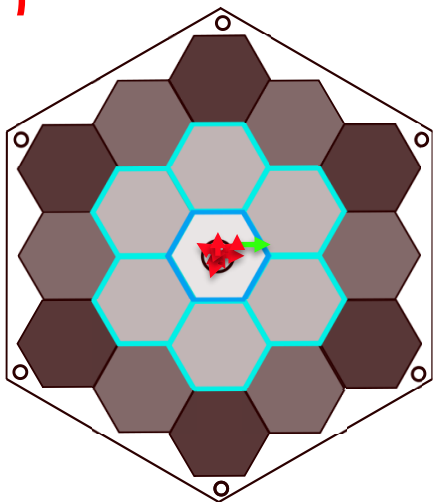
1吨重NaI闪烁体,  
分成19个模块,  
可以同时探测  
 $\beta$ ,  $\gamma$ , n



$\gamma$ 探测效率: ~99%  
 $\beta$ 探测效率: ~30% (5MeV)  
n探测效率: ~15% (<2MeV)

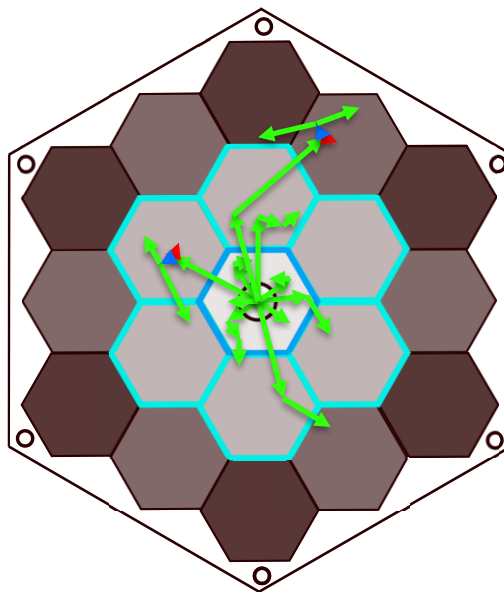


## $\beta$ s in MTAS



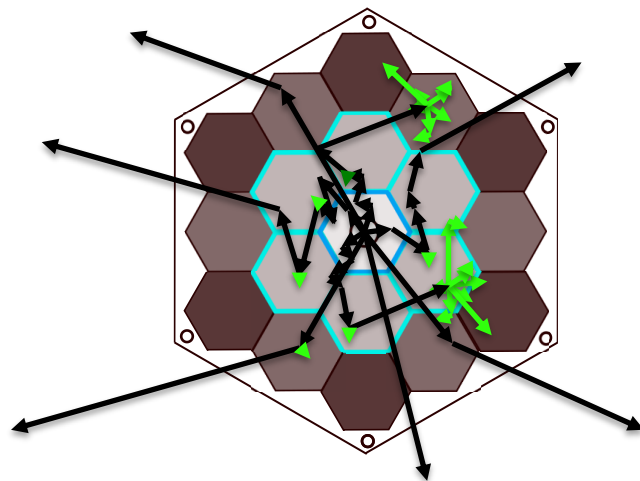
$\beta$ 探测效率:  
~30% (5MeV)

## $\gamma$ s in MTAS

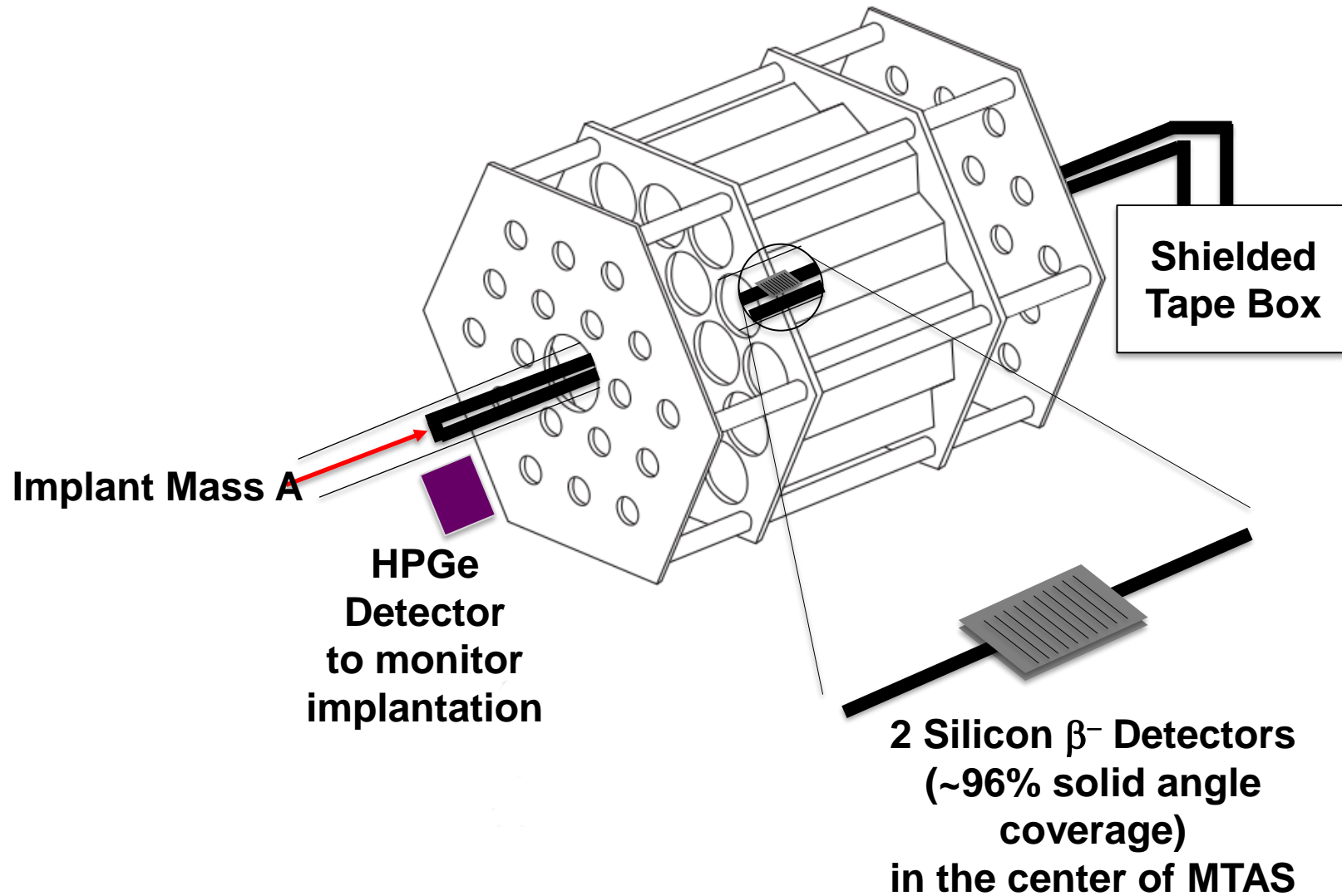


$\gamma$ 探测效率:  
~99%

## Neutrons in MTAS



n探测效率:  
~15% (<2MeV)





## MTAS at CARIBU:

- commissioning run with A = 104 and 105 beams of  $^{252}\text{Cf}$  fission products of refractory elements using ANL's Multi-Reflection Time of Flight spectrometer (MRTOF), Nov. 2019.

- first part of the main experiment on A = 106 and 107 with MRTOF, Feb.-Mar. 2020.

- A = 99, 101, 102 and 132 in Jun. 2021

-  $^{106}\text{Rh}$  and  $^{144}\text{Pr}$  in Sep. 2021

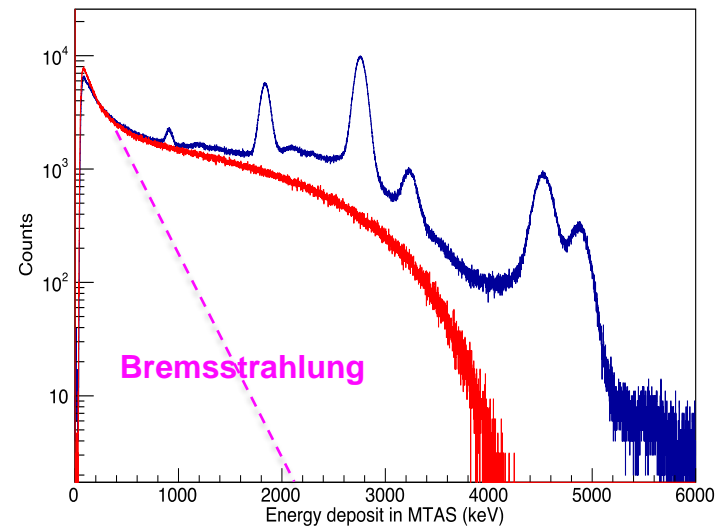
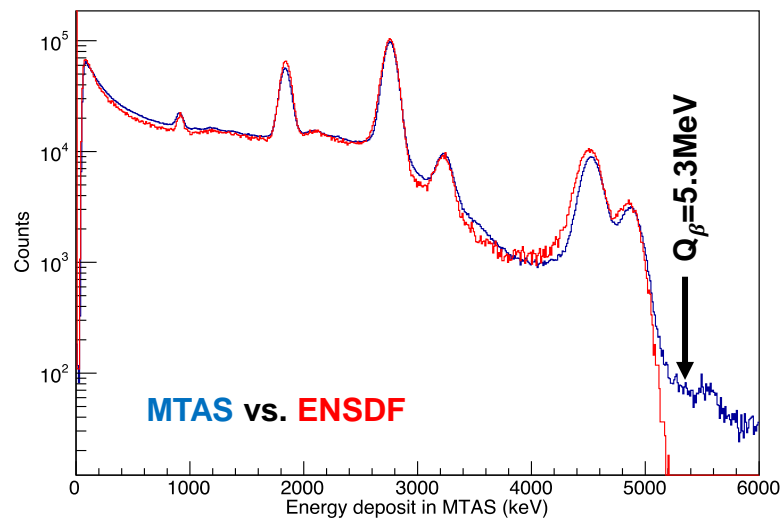
Decays of isotopes marked by green and red ovals were studied during the experiments with MTAS at CARIBU.

Assessment of fission product decay data for decay heat calculations  
2007 NEA Yoshida and Nichols

|                                |                                 |                                 |                                 |                                |                                 |                                |                                |                                |                                 |                                |                                |
|--------------------------------|---------------------------------|---------------------------------|---------------------------------|--------------------------------|---------------------------------|--------------------------------|--------------------------------|--------------------------------|---------------------------------|--------------------------------|--------------------------------|
| $^{101}\text{Pd}$<br>$\beta^+$ | $^{102}\text{Pd}$<br>$2\beta^+$ | $^{103}\text{Pd}$<br>e- capture | $^{104}\text{Pd}$<br>Stable     | $^{105}\text{Pd}$<br>Stable    | $^{106}\text{Pd}$<br>Stable     | $^{107}\text{Pd}$<br>$\beta^-$ | $^{108}\text{Pd}$<br>Stable    | $^{109}\text{Pd}$<br>$\beta^-$ | $^{110}\text{Pd}$<br>$2\beta^-$ | $^{111}\text{Pd}$<br>$\beta^-$ | $^{112}\text{Pd}$<br>$\beta^-$ |
| $^{100}\text{Rh}$<br>$\beta^+$ | $^{101}\text{Rh}$<br>e- capture | $^{102}\text{Rh}$<br>$\beta^+$  | $^{103}\text{Rh}$<br>Stable     | $^{104}\text{Rh}$<br>$\beta^-$ | $^{105}\text{Rh}$<br>$\beta^-$  | $^{106}\text{Rh}$<br>$\beta^-$ | $^{107}\text{Rh}$<br>$\beta^-$ | $^{108}\text{Rh}$<br>$\beta^-$ | $^{109}\text{Rh}$<br>$\beta^-$  | $^{110}\text{Rh}$<br>$\beta^-$ | $^{111}\text{Rh}$<br>$\beta^-$ |
| $^{99}\text{Ru}$<br>Stable     | $^{100}\text{Ru}$<br>Stable     | $^{101}\text{Ru}$<br>Stable     | $^{102}\text{Ru}$<br>Stable     | $^{103}\text{Ru}$<br>$\beta^-$ | $^{104}\text{Ru}$<br>$2\beta^-$ | $^{105}\text{Ru}$<br>$\beta^-$ | $^{106}\text{Ru}$<br>$\beta^-$ | $^{107}\text{Ru}$<br>$\beta^-$ | $^{108}\text{Ru}$<br>$\beta^-$  | $^{109}\text{Ru}$<br>$\beta^-$ | $^{110}\text{Ru}$<br>$\beta^-$ |
| $^{98}\text{Tc}$<br>$\beta^-$  | $^{99}\text{Tc}$<br>$\beta^-$   | $^{100}\text{Tc}$<br>$\beta^-$  | $^{101}\text{Tc}$<br>$\beta^-$  | $^{102}\text{Tc}$<br>$\beta^-$ | $^{103}\text{Tc}$<br>$\beta^-$  | $^{104}\text{Tc}$<br>$\beta^-$ | $^{105}\text{Tc}$<br>$\beta^-$ | $^{106}\text{Tc}$<br>$\beta^-$ | $^{107}\text{Tc}$<br>$\beta^-$  | $^{108}\text{Tc}$<br>$\beta^-$ | $^{109}\text{Tc}$<br>$\beta^-$ |
| $^{97}\text{Mo}$<br>Stable     | $^{98}\text{Mo}$<br>$2\beta^-$  | $^{99}\text{Mo}$<br>$\beta^-$   | $^{100}\text{Mo}$<br>$2\beta^-$ | $^{101}\text{Mo}$<br>$\beta^-$ | $^{102}\text{Mo}$<br>$\beta^-$  | $^{103}\text{Mo}$<br>$\beta^-$ | $^{104}\text{Mo}$<br>$\beta^-$ | $^{105}\text{Mo}$<br>$\beta^-$ | $^{106}\text{Mo}$<br>$\beta^-$  | $^{107}\text{Mo}$<br>$\beta^-$ | $^{108}\text{Mo}$<br>$\beta^-$ |
| $^{96}\text{Nb}$<br>$\beta^-$  | $^{97}\text{Nb}$<br>$\beta^-$   | $^{98}\text{Nb}$<br>$\beta^-$   | $^{99}\text{Nb}$<br>$\beta^-$   | $^{100}\text{Nb}$<br>$\beta^-$ | $^{101}\text{Nb}$<br>$\beta^-$  | $^{102}\text{Nb}$<br>$\beta^-$ | $^{103}\text{Nb}$<br>$\beta^-$ | $^{104}\text{Nb}$<br>$\beta^-$ | $^{105}\text{Nb}$<br>$\beta^-$  | $^{106}\text{Nb}$<br>$\beta^-$ | $^{107}\text{Nb}$<br>$\beta^-$ |
| $^{95}\text{Zr}$<br>$\beta^-$  | $^{96}\text{Zr}$<br>$2\beta^-$  | $^{97}\text{Zr}$<br>$\beta^-$   | $^{98}\text{Zr}$<br>$\beta^-$   | $^{99}\text{Zr}$<br>$\beta^-$  | $^{100}\text{Zr}$<br>$\beta^-$  | $^{101}\text{Zr}$<br>$\beta^-$ | $^{102}\text{Zr}$<br>$\beta^-$ | $^{103}\text{Zr}$<br>$\beta^-$ | $^{104}\text{Zr}$<br>$\beta^-$  | $^{105}\text{Zr}$<br>$\beta^-$ | $^{106}\text{Zr}$<br>$\beta^-$ |
| $^{94}\text{Y}$<br>$\beta^-$   | $^{95}\text{Y}$<br>$\beta^-$    | $^{96}\text{Y}$<br>$\beta^-$    | $^{97}\text{Y}$<br>$\beta^-$    | $^{98}\text{Y}$<br>$\beta^-$   | $^{99}\text{Y}$<br>$\beta^-$    | $^{100}\text{Y}$<br>$\beta^-$  | $^{101}\text{Y}$<br>$\beta^-$  | $^{102}\text{Y}$<br>$\beta^-$  | $^{103}\text{Y}$<br>$\beta^-$   | $^{104}\text{Y}$<br>$\beta^-$  | $^{105}\text{Y}$<br>$\beta^-$  |

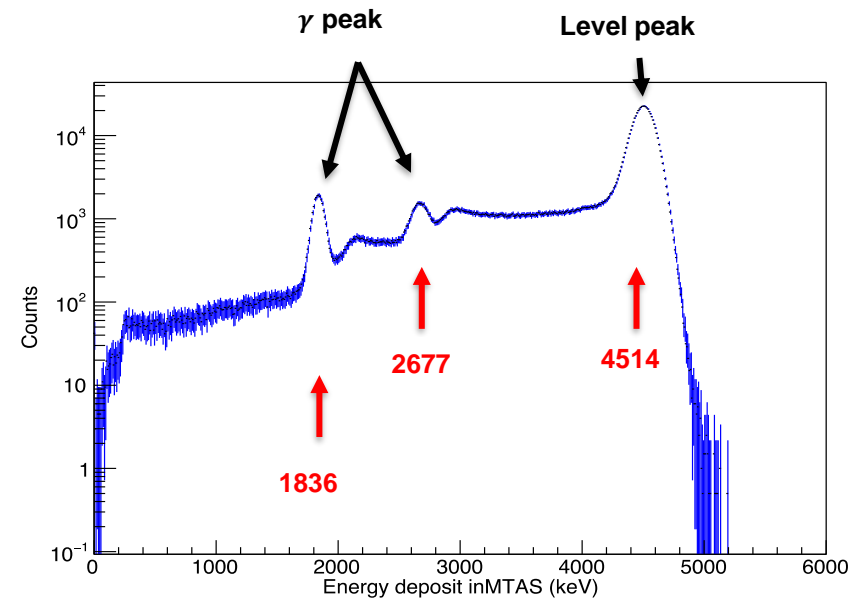
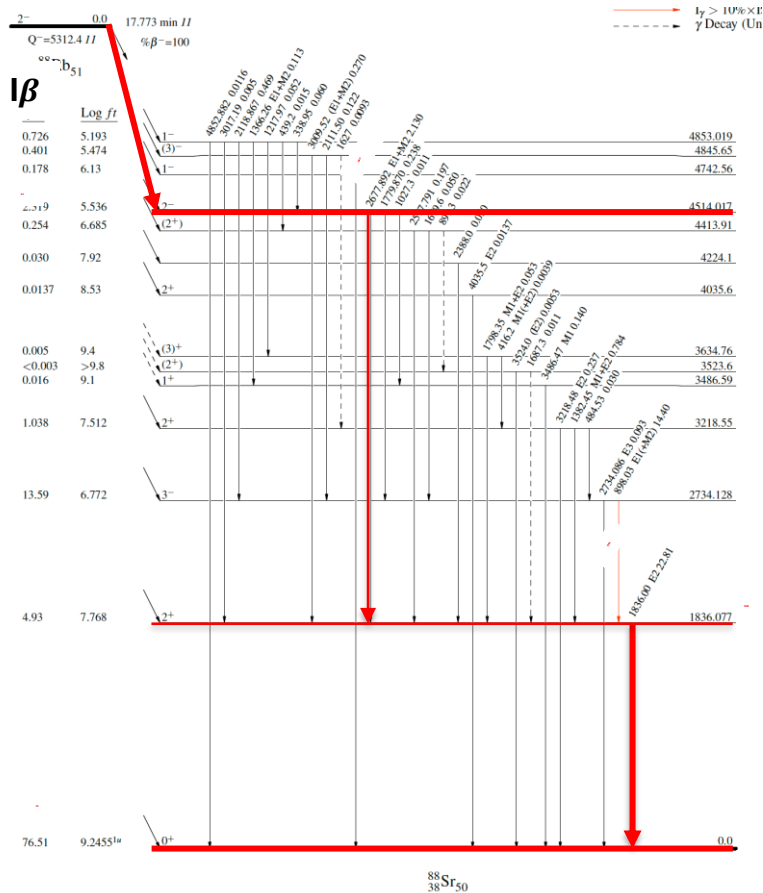
## $^{88}\text{Rb}$ : MTAS response function generated with Geant4

Comparison of simulated nuclear data with  
MTAS experimental spectrum



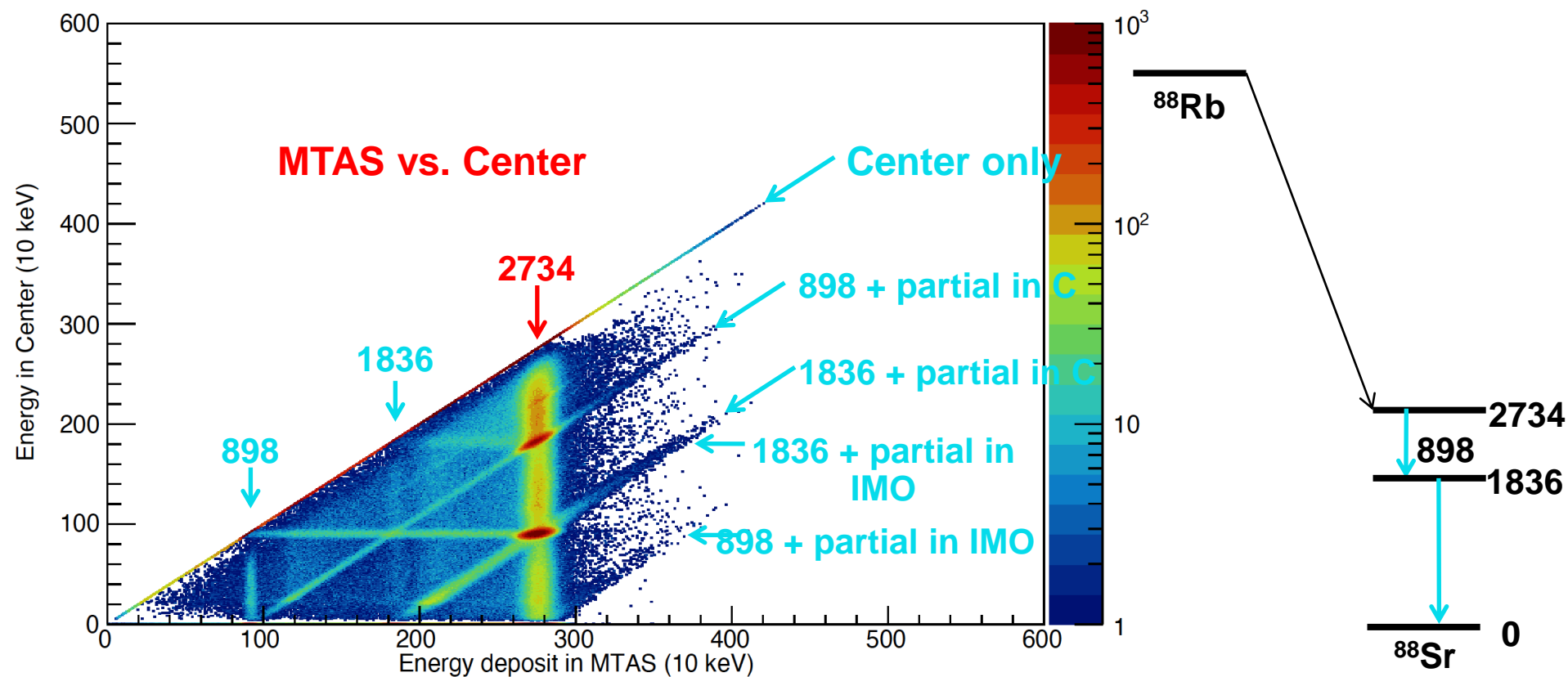
## $^{88}\text{Rb}$ : MTAS response function generated with Geant4

An example of “decay path”





# MTAS vs. Center 响应函数







# 响应函数矩阵和解谱算法

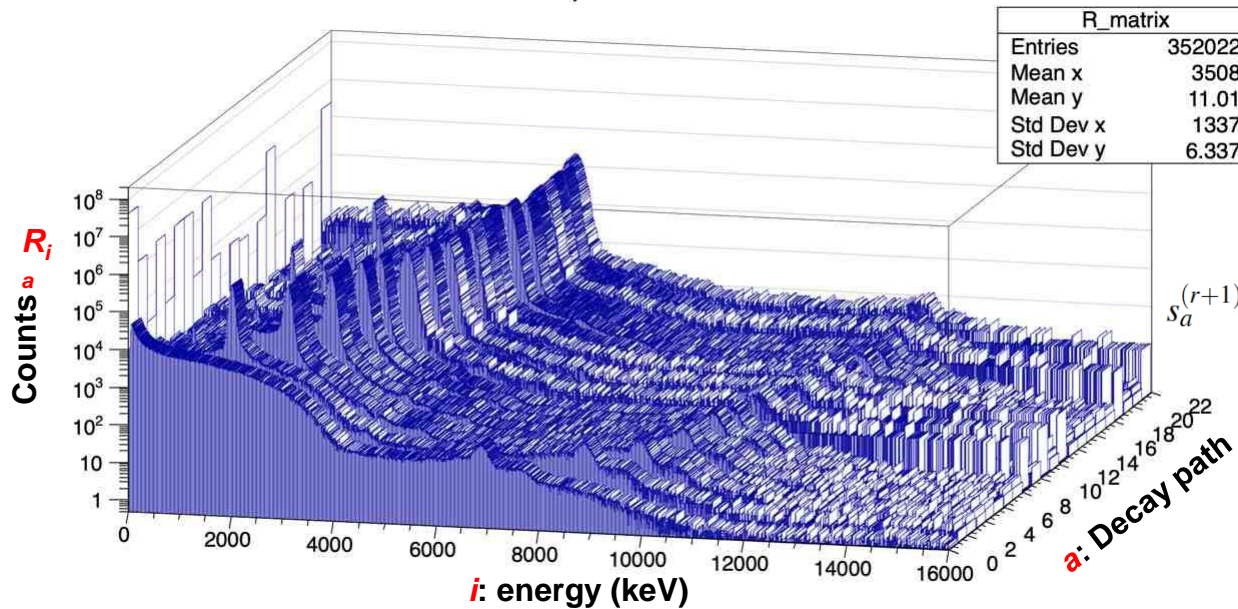


## 1-D MTAS response functions ( $^{88}\text{Rb}$ )

$$d = R \cdot s$$

Response function

Expectation-Maximization Method:



普适  
健壮  
可扩展

$$s_a^{(r+1)} = \frac{1}{\sum_{k=1}^N R_{ka}} \sum_{i=1}^N \frac{R_{ia} s_a^{(r)} d_i}{\sum_{b=1}^M R_{ib} s_b^{(r)}}, \quad a = 1, \dots, M.$$

$$I_a = \frac{s_a}{\sum_{a=1}^M s_a}, \quad a = 1, \dots, M,$$

$d_i$  from the experimental data: total MTAS spectrum

$R_{ia}$  is normalized to the 1M events in geant4 sim for each decay path

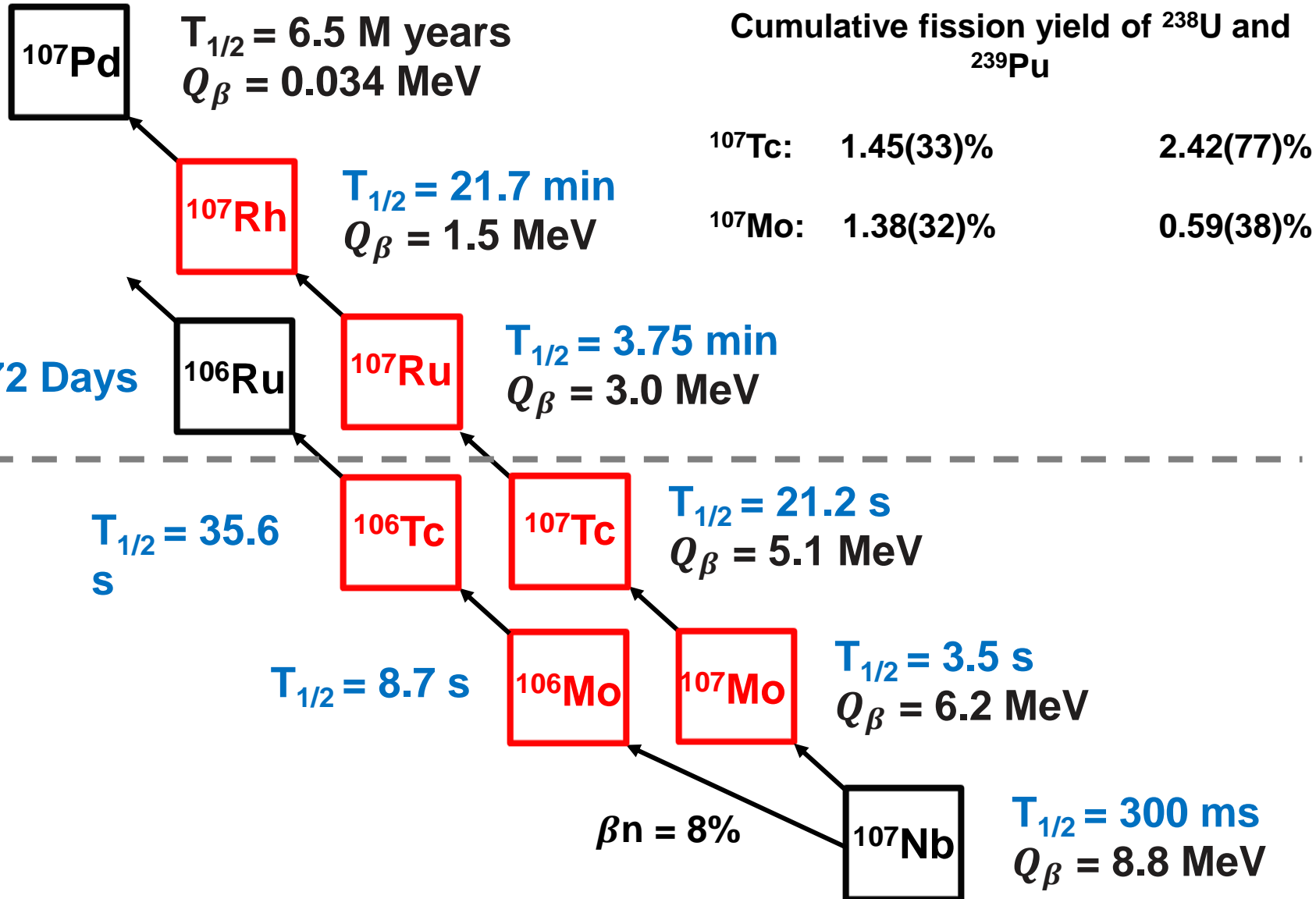
L.B. Lucy, Astron. J. 79 (1974) 745.

P. Shuai et al. Phys. Rev. C 105, 054312 (2022)

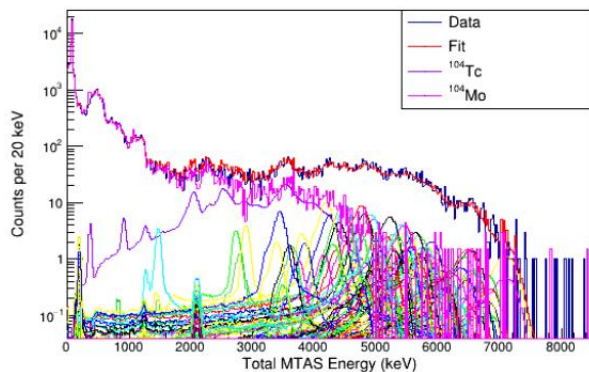




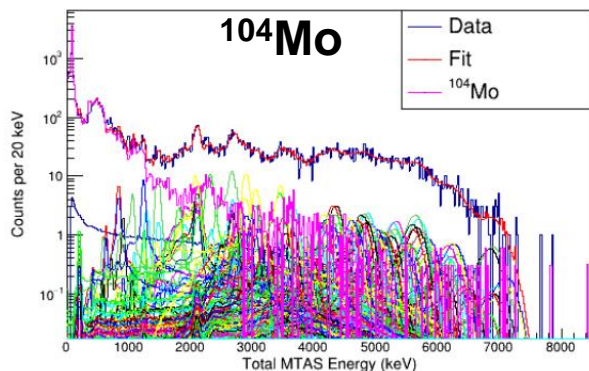
# A=107衰变链



$^{104}\text{Tc} + ^{104}\text{Mo}$

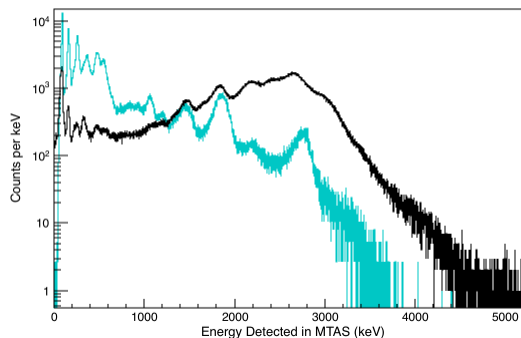


$^{104}\text{Mo}$



Preliminary

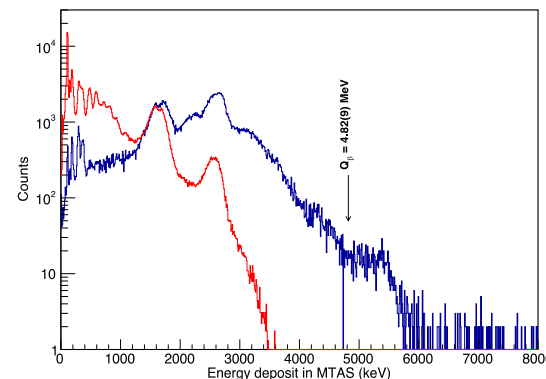
$^{105}\text{Mo}$



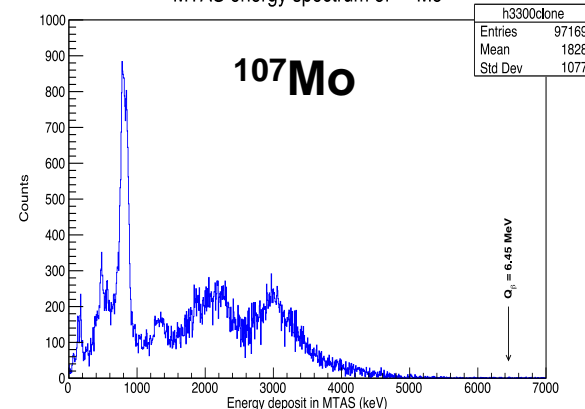
**Pandemonium Effect  
普遍存在!**

$^{107}\text{Tc}$

MTAS Spectrum of  $^{107}\text{Tc}$  vs. ENSDF



MTAS energy spectrum of  $^{107}\text{Mo}$



**24.4% excess of  $\nu$  flux at energy 8-8.5MeV reported by Daya Bay**

Daya Bay collaboration, Phys. Rev. Lett. 129, 041801 (2022)

**This work: the excess increase to 28.5% (to be submitted)**



# Decay Heat



| $\beta$ decay heat | MTAS (MeV) | $\gamma$ decay heat | ENSDF (MeV) | MTAS (MeV) |
|--------------------|------------|---------------------|-------------|------------|
| $^{107}\text{Rh}$  | 0.462      | $^{107}\text{Rh}$   | 0.308       | 0.184 ↓    |
| $^{107}\text{Ru}$  | 0.995      | $^{107}\text{Ru}$   | 0.382       | 0.341 ↓    |
| $^{107}\text{Tc}$  | 1.05       | $^{107}\text{Tc}$   | 0.553       | 2.2(1) ↑   |
| $^{107}\text{Mo}$  | 1.8        | $^{107}\text{Mo}$   | N/A         | 1.9(1)     |

Cumulative fission yield of  $^{238}\text{U}$  and  $^{239}\text{Pu}$

$^{107}\text{Tc}$ : 1.45(33)% 2.42(77)%

$^{107}\text{Mo}$ : 1.38(32)% 0.59(38)%

$^{107}\text{Tc}$ : MTAS:  $E_{\gamma}=2.2(1)$  MeV

Algora:  $E_{\gamma}=1.822(450)$  MeV.

A. Algora, PRL 105, 202501 (2010)



# 总结



- $\beta$ 衰变在核物理，反应堆物理和中微子物理中起到关键作用。
- 全吸收谱仪可以克服Pandemonium效应，得到真实的 $\beta$ 衰变分支比 $I_\beta$
- $A=104, 105, 107$ 的 $\beta$ 衰变链中都发现Pandemonium效应的影响， $^{104}\text{Nb}$ 导致中微子能谱在8-8.5MeV的理论计算和实验值相差更多。
- 更多Pandemonium free的核数据需要用TAS重新测量

## MTAS Collaboration March 2020 at Argonne National Laboratory

